Prediction of nanomagnetite stoichiometry (Fe(II)/Fe(III)) under contrasting pH and redox conditions

Phoomipat Jungcharoen, Mathieu Pédrot, Frank Heberling, Khalil Hanna, Fadi Choueikani, Charlotte Catrouillet, Aline Dia, Remi Marsac

View Article Online
View Journal

Environmental Science Nano

Accepted Manuscript

This article can be cited before page numbers have been issued, to do this please use: P. Jungcharoen, M. Pédrot, F. Heberling, K. Hanna, F. Choueikani, C. Catrouillet, A. Dia and R. Marsac, *Environ. Sci.: Nano*, 2022, DOI: 10.1039/D2EN00112H.

View Article Online
DOI: 10.1039/D2EN00112H

Prediction of nanomagnetite stoichiometry (Fe(II)/Fe(III)) under contrasting pH and redox conditions

Phoomipat Jungcharoen[1,2], Mathieu Pédrot[1], Frank Heberling[3], Khalil Hanna[4], Fadi Choueikani[5], Charlotte Catrouillet[1], Aline Dia[1], Rémi Marsac[1]*

[1] Univ. Rennes, CNRS, Géosciences Rennes – UMR 6118, F-35000 Rennes, France.
[2] Department of Environmental Engineering, Faculty of Engineering and Research Center for Environmental and Hazardous Substance Management, Khon Kaen University, Khon Kaen 40002, Thailand
[3] Institute for Nuclear Waste Disposal, Karlsruhe Institute of Technology, P.O. Box 3640, D-76021 Karlsruhe, Germany
[4] Univ Rennes, Ecole Nationale Supérieure de Chimie de Rennes, CNRS, ISCR-UMR 6226, F-35000, Rennes, France.
[5] Synchrotron SOLEIL, L'Orme des Merisiers, Saint- Aubin BP48, 91192 Gif-sur- Yvette cedex, France.

* Corresponding author: E-mail: remi.marsac@univ-rennes1.fr

View Article Online
DOI: 10.1039/D2EN00112H

Abstract

Magnetite ($Fe(III)_2Fe(II)O_4$) nanoparticles are fascinating nanoparticulate minerals for their electronic, magnetic and chemical properties. Ubiquitous, in the environment, they are also among the most used ferromagnetic nanomaterials in environmental, industrial and biomedical applications. Their intriguing structural and reactivity features do not only arise from the "nano-effect" but also, from the occurrence of Fe^{2+} ions in their structure. Previous studies showed that partial oxidation of (nano)magnetite may occur. However, such transformations were only monitored under either oxidizing or very acidic conditions. Here, we report that 10 nm-sized stoichiometric magnetite particles (Fe(II)/Fe(III) = 0.5) are in fact not stable in aqueous solutions over a biologically- and environmentally- relevant pH range (4-7). In the absence of O_2, an H^+-promoted dissolution process is responsible for the preferential release of Fe(II) into solution, which leads to partial oxidation of magnetite to a magnetite-maghemite solid-solution. Long-term kinetic investigations combined with XMCD measurements reveal that the dynamic exchange of Fe(II) between the surface and the solution is key in determining the magnetite stoichiometry even at circumneutral pH. Based on this finding, we developed a thermodynamic model for the magnetite-maghemite solid-solution able to predict the chemical stability of the 10 nm-sized magnetite. This model enables to rationalize and predict the behavior and transformation of magnetite nanoparticles in aqueous solutions, which is crucial for a broad range of applications (medicine, biology, chemistry, environment, etc.).

Environmental significance

Magnetite nanoparticles are highly reactive ubiquitous nanominerals in natural systems, which control the behavior and fate of many contaminants. However, their reactivity depends on the composition, especially their Fe(II) and Fe(III) content. Therefore, it is crucial to understand and predict the effect of various factors on magnetite stoichiometry (Fe(II)/Fe(III)), as it is known to vary greatly in aquatic environments. This work focuses on two of the most important abiotic processes controlling magnetite stoichiometry, namely the oxidation of Fe(II) to Fe(III) and the preferred release of Fe(II) over Fe(III) to the solution at acidic pH. It provides the first predictive model of nanomagnetite stoichiometry under various pH and redox conditions, which could be used to unravel the complex behavior and reactivity of these nanomaterials in contrasted environmental settings.

View Article Online
DOI: 10.1039/D2EN00112H

1 Introduction

Magnetite is a mixed-valence iron oxide with an inverse spinel structure, which is commonly found at a nanometric size in soils and sediments. Its formula is $[Fe^{2+}\ Fe^{3+}]_{Oh}\ Fe^{3+}_{Td}\ O_4^{2-}$, where high spin Fe^{2+} and Fe^{3+} can be found in octahedral (Oh) and tetrahedral (Td) coordination. However, magnetite can be partially or entirely oxidized into the isostructural mineral-phase, maghemite (Fe_2O_3 or $[Fe^{3+}_{5/3}\square_{1/3}]_{Oh}Fe^{3+}_{Td}\ O_4^{2-}$), containing vacant Oh sites (□) instead of Fe^{2+}. Magnetite, maghemite and intermediate phases are characterized by the Fe(II)/Fe(III) ratio, denoted R, ranging from 0 (pure maghemite) to 0.5 (pure magnetite).[1–3] The occurrence of Fe^{2+} ions in the magnetite structure gives rise to its unique electronic and magnetic properties, and makes it a key-ingredient in a wide range of applications in catalysis, biomedical and environmental chemistry.

On one hand side, the redox sensitivity of magnetite is problematic for many applications, because it depends on the mixing of iron valence states in the crystal structure. For instance, the high bulk electron conductivity of magnetite is only possible due to the fast electron hopping between Fe^{2+} and Fe^{3+} ions on Oh sites,[4] or the strong magnetic moment of magnetite fully depends on the presence of Fe^{2+}, because the magnetic moments of both types of Fe^{3+} ions cancel each other.[1] In such cases, Fe^{2+} release or its oxidation to Fe^{3+} may impede magnetite applicability.

On the other hand side, the redox properties make magnetite excellent "batteries" for both human activities[5] and microorganisms,[6] and are responsible for the reduction or oxidation of redox-sensitive chemical compounds at the magnetite surface in industrial and environmental processes.[2,7–12] or in medical applications.[13,14] For instance, the impact of the stoichiometry of nanomagnetite on the thermodynamics and kinetics of the reduction reactions of inorganic and organic compounds has been investigated for U(VI) reduction to U(IV)[8] and for nitrobenzene reduction to aniline[7]. The adsorption of organic contaminants (e.g. quinolone antibiotics)[15] was also shown to increase with R, which could have a drastic effect on the fate and behavior of such contaminants in natural systems. For these reasons, it appears crucial to understand and predict the impact of physico-chemical conditions on magnetite stoichiometry.

The oxidation of magnetite to maghemite is well documented and, in the presence of O_2, can be formulated as:

$$4\ Fe_3O_{4(s)} + O_{2(g)} \rightleftharpoons 6\ Fe_2O_{3(s)} \qquad (1)$$

View Article Online
DOI: 10.1039/D2EN00112H

Another transformation reaction of magnetite to maghemite involves its H^+-promoted dissolution, which releases Fe^{2+} ions into the solution, leaves Fe^{3+} in the solid phase and does not require O_2 as an oxidant:

$$Fe_3O_{4(s)} + 2\ H^+_{(aq)} \rightleftharpoons Fe_2O_{3(s)} + Fe^{2+}_{(aq)} + H_2O_{(l)} \quad (2)$$

This reaction is highly relevant for many applications of magnetite nanoparticles in aqueous suspensions, e.g. medicine,[13,14] biology,[6,16] chemistry,[17,18] environment,[19,20] Unfortunately, the transformation of nanomagnetite into non-stoichiometric nanomagnetite via equation 2 has only been characterized in acidic solutions (e.g. pH < 3),[21,22] with large magnetite particles (> 100 nm),[23] at high temperature,[24] or in presence of O_2.[19] Knowledge on the magnetite stability and reactivity under low O_2 content and slightly acidic to circumneutral pH is scarce, even though these conditions are very often encountered in biological media or subsurface environments. Previous reports have either limited investigations on the magnetite reactivity to neutral and alkaline conditions under O_2-free atmosphere (e.g.[7,8,10,15,25]), or overlooked Fe^{2+} release at low pH through the chemical transformation of magnetite, which occurs under these conditions (e.g. [9,12,26]). In addition, because slow processes can be observed, only the kinetic aspects of equation 2 were treated.[23] This is problematic, especially in natural systems experiencing large fluctuations of the local pH and redox conditions, because equilibrium data are also required for the prediction of magnetite stoichiometry. Given the extensive use of magnetite nanoparticles and their importance in a biological and environmental context, it becomes urgent to fully characterize the impact of physico-chemical conditions, and especially the pH on magnetite stoichiometry, and the consequences on magnetite redox and surface reactivity in aqueous systems.

In the present work, an extensive dataset on the solubility of magnetite nanoparticles (10 nm-sized) in aqueous suspension is presented. Long-term kinetic investigations (up to 560 days) shed light on overlooked aspects of the dissolution processes and whether chemical equilibrium can be reached under controlled laboratory conditions. Based on these data the first chemical thermodynamic model for nanosized magnetite stoichiometry in aqueous solutions is developed, capable of predicting the composition of the investigated nanomagnetites as a function of solution chemistry (i.e. dissolved Fe^{2+} concentration, pH, and redox potential). Given the extensive use of magnetite nanoparticles in biological and environmental sectors, this model will help in examining and predicting the reactivity of either natural magnetite nanoparticles or engineered ones prior to technological applications.

View Article Online
DOI: 10.1039/D2EN00112H

2 Materials and methods

2.1 Chemicals.

Iron(III) chloride hexahydrate ($FeCl_3 \cdot 6H_2O$), Iron(II) chloride tetrahydrate ($FeCl_2 \cdot 4H_2O$), and NaCl were purchased from AnalaR NORMAPUR. Hydrogen peroxide (H_2O_2), hydrochloric acid (HCl), sodium hydroxide (NaOH), and sodium citrate were obtained from Sigma-Aldrich. The sample solutions were prepared with ultrapure "MilliQ" water (specific resistivity 18.2 $M\Omega cm^{-1}$). All experiments were carried out in an anaerobic chamber (N_2-glovebox, JACOMEX) and all solutions were purged from $O_{2(g)}$ prior to use. All pH adjustments were done by HCl and NaOH addition (no buffer was used).

2.2 Synthesis of magnetites with various stoichiometries.

Magnetite nanoparticles (10 nm) preparation was described previously.[27] Samples used in the present study come from the same batch. The synthesis procedure is repeated for clarity. The procedure involves a room temperature aqueous precipitation.[27,28] Briefly, a 0.5 M HCl solution (40 mL) containing a 0.5 M $FeCl_2$ and 1 M $FeCl_3$ (1:2 molar ratio) was added dropwise into a 0.5 M NaOH solution (250 mL) with continuous stirring, leading to instantaneous precipitation of magnetite particles. After the synthesis, the pH of the suspension was adjusted to 8.5. Then, the solid phase was washed three times with ultrapure water at pH 8.5 (adjusted using NaOH) to avoid any Fe^{2+} release, as observed in previous work,[15,29] and thus, to guarantee the stoichiometry of R0.5. Known amounts of H_2O_2 were added to R0.5 to produce defined non-stoichiometric magnetite (R0.1, R0.2, R0.3, R0.4) sets.[15,27] Then, mother solutions were replaced with ultrapure water (at pH = 8.5) in order to remove residual H_2O_2. Initial Fe(II)/Fe(III) ratios (R_{ini}) of these (non)-stoichiometric magnetites were determined by acid digestion in 0.6 M HCl during 3 days, followed by spectrophotometric determination of dissolved [Fe(II)] and total [Fe] (= [Fe(III)] + [Fe(II)]) using the 1-10 phenantroline colorimetric method,[30] as well as by X-ray Magnetic Circular Dichroism (XMCD).[27] Results were in excellent agreement with expected values from the amount of H_2O_2 added, as expected from previous studies.[15,27,31] Acid digestion followed by spectrophotometry was repeated three times for R0.5 and each non-stoichiometric magnetite, which led to an error of ±0.01 on the determination of R_{ini}. This error is consistent with previous work.[32]

View Article Online
DOI: 10.1039/D2EN00112H

2.3 Batch studies.

All experiments were conducted with 10 mM NaCl as background electrolyte. Fe dissolution kinetic studies were at pH 4, 5.5 and 8 for R_{ini} = 0.5, and at pH 4 for R_{ini} = 0.10 and 0.30. Iron total concentration in the suspensions was 6.5 mM, corresponding to ~0.5 g L^{-1} of magnetite, in 100 mL suspensions in 250 mL HDPE bottles. pH was controlled and regularly adjusted over a 560-days period using HCl and NaOH. Equilibrium studies were conducted in 10 mM NaCl solutions and in 15 mL polypropylene tubes containing 10 mL of solution. Reaction time was 20 days (for R_{ini} = 0.50), 60 days (R_{ini} = 0.30, 0.40) or 320 days (R_{ini} = 0.10, 0.20). The impact of dissolved Fe(II) addition on the recharge of R0.1 was investigated by adding small amounts of a 100 mM $FeCl_2$ solution. The impact of the presence of an excess of Fe(II) or citrate on R0.5 was investigated by adding 0.25, 0.5 or 1 mM Fe^{2+}, or 1 mM citric acid to R0.5. After a given reaction time, pH and redox potential (E_H) were measured and the suspension was passed through a 0.2 µm cellulose acetate filter (Sartorius Minisart), followed by dissolved [Fe(II)] and [Fe(III)] determination by spectrophotometry. Citrate-containing samples were ultrafiltered at 5kDa (Vivaspin 15RH12, Sartorius). The absence of Fe nanoparticles in the filtrate was checked by Dynamic Light Scattering (VASCO Flex).

The effective stoichiometry of magnetite (R_{eff}) was calculated from the initial stoichiometry (R_{ini}), the total concentration of Fe(III) in both the aqueous and solid phases ($[Fe(III)]_{tot}$) and the measured aqueous Fe^{2+} concentration ($[Fe(II)]_{aq}$):

$$R_{eff} = R_{ini} - \frac{[Fe(II)]_{aq}}{[Fe(III)]_{tot}} \quad (3)$$

By assuming 5% uncertainty on $[Fe(II)]_{aq}$ determination by spectrophotometry, and accounting for the uncertainty on R_{ini}, we determine that the error on R_{eff} was comprised between 0.01 and 0.03.

pH and E_H were recorded in both magnetite and Fe(II)-amended magnetite suspensions using a multiparameter electrode (pH, E_H and T; Hach, sensION+5045). The pH electrode was calibrated with 3 standard buffers (pH 4, 7, and 10). The Pt electrode combined with a Ag/AgCl reference electrode, used for redox potential measurements, was calibrated using a commercial redox buffer (220 mV vs Ag/AgCl). Raw data were converted into E_H vs standard hydrogen electrode (SHE) by correcting for the potential of the reference electrode. An equilibration time of 15 minutes was applied for all E_H measurements. The suspension was stirred prior to the E_H measurements. The electrode surface was periodically cleaned by exposing it to 0.1 M HCl for 1 h.

View Article Online
DOI: 10.1039/D2EN00112H

2.4 Characterization by TEM and XMCD.

Transmission Electron Microscopy (TEM; Jeol JEM 1230 microscope) was used for characterization of magnetite nanoparticles. Briefly, A small aliquot of magnetite suspension was diluted with ultrapure water and sonicated for 20 min. A droplet of the diluted suspension was deposited on a carbon-coated 200-mesh copper grid and dried inside the anaerobic chamber. Samples were transported to the microscope in an N_2 atmosphere using a hermetic holder and the samples were analyzed at an acceleration voltage of 200 kV. Average particle diameters were determined by measuring 100 particles.

XMCD signals were recorded at the Fe $L_{2,3}$ edges (700 – 730 eV) on the DEIMOS beamline at the synchrotron light source SOLEIL as previously described.[27,33,34] Briefly, samples were transported to the SOLEIL Synchrotron facility at the DEIMOS beamline in 1 mL tubes, placed in airtight bottles that had been closed in the N_2-glovebox. Colloidal suspensions of nanoparticles were drop-casted on silicon substrates and dried at room temperature, in an Ar-glove box ($O_{2(g)}$ < 1 ppm) connected to the end station. The silicon substrates were fixed on a sample holder and transferred into the cryomagnet, under ultra-high vacuum (UHV-10^{-10} mbar). All spectra were measured in Total Electron Yield mode (TEY) at 4.2 K under UHV conditions and an applied magnetic field H (H^+ = +6 Tesla and H^- = -6 Tesla). The beam size was 800*800 μm^2 and the resolution was 100 meV. XMCD spectra were plotted by considering the absorption cross-section measured with left (σ_L) and right (σ_R) circularly polarized X-rays. XMCD spectra were plotted as $\sigma_{XMCD} = (\sigma_+ - \sigma_-)$ where $\sigma_+ = [\sigma_L(H^+) + \sigma_R(H^-)]/2$ and $\sigma_- = [\sigma_L(H^-) + \sigma_R(H^+)]/2$. The circularly polarized X-rays are provided by an Apple-II HU-52 helical undulator for XMCD measurements and by sweeping the magnetic field from +6T to -6T. XMCD signals were normalized by dividing the raw signal by the height of the maximum.

2.5 Aqueous speciation modeling

PHREEQC (version 2)[35] is a computer code based on an ion-association aqueous model, which was designed to perform speciation and saturation-index calculations in water. Davies equation was used for activity coefficients calculation, being valid up to an ionic strength of 0.1 M. PhreePlot[36] contains an embedded version of the geochemical speciation program PHREEQC. It includes a parameter optimization procedure, which automatically adjusts a model to experimental data by minimizing the weighted sum of squares of the residuals.

View Article Online
DOI: 10.1039/D2EN00112H

3 Results

3.1 Time dependent Fe^{2+} release from magnetite.

When maintaining stoichiometric magnetite nanoparticles (0.5 g L^{-1}) at pH = 8 in 10 mM NaCl solution, a marginal release of Fe into solution is observed, evidencing the stability of magnetite at these conditions. By contrast, at pH = 5.5, a fast release of Fe^{2+} occurs already after 1 day, while aqueous Fe^{3+} is not detectable. This incongruent dissolution process impacts the effective stoichiometry of magnetite (R_{eff}; Fig. 1a). Accordingly, R_{eff} drops from 0.50 to 0.36 within 1 day, and then remains constant over time, suggesting the establishment of a chemical equilibrium.

Exposing nanomagnetite to a pH 4 solution leads to a rapid release of Fe^{2+} within the first two days, with a concomitant decrease of R_{eff} from 0.50 to ca. 0.20. The dissolution process slows down when R_{eff} approaches 0.10, but it seems to tend to 0 over time scales much longer than that of this study ~1.5 year (540 days) (Fig. 1a). The experiments on Fe(II) release from stoichiometric magnetite are complemented by experiments using nanomagnetites of defined stoichiometries (R_{ini} = 0.10, 0.30 and 0.50) (Fig. 1b). Here, a fast initial Fe^{2+} release was observed for R_{ini} = 0.30 then, the reaction slowed down when R_{eff} approached 0.10, whereas the process was slow from the beginning in the experiment for R_{ini} = 0.10. As previously suggested in the literature[37] the initial release of Fe(II) from the near surface region may be fast due to electron transfer from the interior of the particle to the surface. This, however, causes a charge imbalance inside the particle, which must be compensated by the movement of Fe-ions and concomitant generation of octahedral vacancies. Recent diffraction investigations[22] demonstrated oxidation-induced strain in magnetite particles, an effect that likely correlates with this interpretation. This process slows down further with time, also in agreement with an alternative conceptual model, where a Fe(II)-depleted outer rim grows thicker while the core shrinks.[19,23]

3.2 Characterization of the reaction products of magnetite with H^+, H_2O_2 or Fe^{2+}.

As previously shown for the same magnetite batch,[27] the particle size and shape did not evolve much between the pristine stoichiometric magnetite maintained at pH = 8 during 20 days (R_{ini} = 0.50; Fig. 2a), oxidized by H_2O_2 (e.g. R_{ini} = 0.10; Fig. 2c) and subsequently recharged with dissolved Fe^{2+} (Fig. 2d). Maintaining pristine stoichiometric magnetite at pH = 4 during 20 days (R_{eff} = 0.13; Fig. 2b) also gave similar particle size and shape (see Table S2). The structure of these nanomagnetites were probed by synchrotron X-ray magnetic

View Article Online
DOI: 10.1039/D2EN00112H

circular dichroism (XMCD) spectroscopy, which enables to distinguish Fe^{2+}_{Oh}, Fe^{3+}_{Td} and Fe^{3+}_{Oh} according to their distinct characteristic peaks (Fig. 3).[38] The intensity of the Fe^{2+}_{Oh} peak relative to that of Fe^{3+}_{Td} and Fe^{3+}_{Oh} decreases with decreasing pH or after oxidation of the pristine magnetite with H_2O_2 at pH 8. XMCD spectra of magnetite exposed to H_2O_2 and showing R_{ini} = 0.10 and 0.30 are quite similar to those of stoichiometric magnetite equilibrated at pH 4 and 5.5 during 20 days. As observed in previous studies, a complete Fe^{2+} uptake proceeds within less than 1 day when equilibrating a non-stoichiometric magnetite (R_{ini} = 0.10) at pH = 7 with an appropriate amount of dissolved Fe^{2+} to fully restore R_{eff} = 0.50.[7,15,31] Although Fe^{2+} uptake by oxidized magnetite leads to surface recrystallization,[27] it was previously shown that nanomagnetites experiencing oxidation and subsequent Fe^{2+}-recharge reacted similarly to the pristine nanomagnetite concerning contaminant reduction[7] and surface complexation.[15] All these observations suggest that the release-recharge process of Fe^{2+} from magnetite is reversible.

3.3 Combined effects of pH and oxidation on magnetite stoichiometry.

The apparent establishment of an equilibrium at pH ≥ 5.5 after one day (which might be generalized to pH ≥ 5 after 20 days)[39] and the similar reaction products of magnetite with H^+, H_2O_2 or Fe^{2+} further motivated investigation of the magnetite phase-stability at chemical equilibrium. Stoichiometric nanomagnetite suspensions (0.5 g L^{-1}) were equilibrated at different pH values during 20 days (Fig. 4a, in black). In agreement with equation 2, the concentration of Fe(II) released in solution increases with decreasing pH, and R_{eff} decreases from 0.50 at pH = 7 to 0.13 at pH = 5.3. The XMCD spectra were treated using a linear combination fit involving magnetite and maghemite references[27] to calculate R_{eff}. Spectroscopic results were found in excellent agreement with wet chemical analysis (large diamonds in Fig. 4a). These results further confirmed that magnetite nanoparticles cannot be considered as stoichiometric after contact with aqueous solution under acidic conditions, even at moderate acidity (5.3 < pH < 7). Attempts to maintain magnetite stoichiometry at a value of 0.50 by supersaturating the system failed:

(i) working with 5 times more concentrated magnetite suspensions (2.5 g L^{-1}), similar R_{eff} values are obtained although about 5 times larger $[Fe(II)]_{aq}$ are measured (Fig. 4a, in red). If this result is unexpected for a pure phase, it supports the hypothesis that magnetite-maghemite system should be treated as a solid solution. In the first case, $[Fe(II)]_{aq}$ is not supposed to increase with the solid content because the activity

View Article Online
DOI: 10.1039/D2EN00112H

coefficient of a pure phase equals one. Whereas, the activity coefficients or solid solution differs from one, which allows $[Fe(II)]_{aq}$ to increase with the solid content.[40]

(ii) addition of an excess of dissolved Fe(II) (0.25-1 mM) to a stoichiometric magnetite does not significantly affect R_{eff} at pH < 7 (Fig. S1). In fact, much larger $[Fe(II)]_{aq}$ would be required to shift equilibria, but it could also lead to Fe(II)-(hydr)oxide precipitation, as previously observed.[27]

In addition, attempts to coat the surface with an organic ligand such as citrate (1 mM), often used as surfactant to increase the colloidal stability of magnetite, to protect it from oxidation or to reduce its cytotoxicity,[14,41] did not inhibit Fe^{2+} release. Although citrate adsorption occurred, Fe^{2+} complexation by the remaining fraction of citrate in solution leads to a slightly enhanced Fe^{2+} release (Fig. S2). One of the most important conclusions from these experiments is that in all the experiments at pH < 7, suspensions are composed of non-stoichiometric magnetites nanoparticles in solutions containing significant concentrations of dissolved Fe(II).

We further investigated the behavior of magnetites exhibiting different initial stoichiometries (R_{ini} = 0.10, 0.20, 0.30, 0.40 and 0.50) obtained from the original stoichiometric magnetite sample by addition of H_2O_2. As for R_{ini} = 0.50, H^+-promoted Fe^{2+} release leads to a decrease of R_{eff} with decreasing pH (Fig. 4b). Interestingly, R_{eff} values of all initial magnetites follow the same trend, once pH falls below a certain value (e.g. at pH < 5.5, R_{eff} values are equal for magnetites with R_{ini} = 0.30, 0.40 and 0.50), evidencing the strong relationship between R_{eff}, pH, and aqueous Fe^{2+} concentrations. This also suggests fully reversible release/uptake of Fe(II) by magnetite, which was further confirmed over a large pH range by adding Fe^{2+} to a suspension of non-stoichiometric magnetite (R_{ini} = 0.10). Consistently, final R_{eff} values did not significantly differ from the original stoichiometric magnetite (Fig. 4b).

3.4 Chemical thermodynamic modeling of the magnetite-maghemite system.

If variations of magnetite stoichiometry with pH and redox conditions cannot be avoided, quantitative prediction of this phenomenon becomes crucial. For this purpose, we consider non-stoichiometric magnetite as a binary solid-solution between maghemite and magnetite. The Gibbs free energies of formation of the solid-solution ($\Delta G_{ss,nano}$) of magnetite (mt)-maghemite (mm) nanoparticles is expressed by:

$$\Delta G_{ss,nano} = X\Delta G_{mt,nano} + (1-X)\Delta G_{mm,nano} + \Delta G_{mix} \quad (4)$$

View Article Online
DOI: 10.1039/D2EN00112H

The excess free energy of mixing (ΔG_{mix}) can be expressed according to Guggenheim's expansion series:

$$\Delta G_{mix} = X(1-X)RT(a_0 + a_1(2X-1) + \ldots.) \quad (5)$$

Where a_0, a_1, etc. are adjustable non-dimensional Guggenheim parameters.[40] However, in order to describe the thermodynamic equilibrium between a magnetite-maghemite solid-solution and an aqueous solution with the Guggenheim equation, it is necessary to ensure that (i) one ion on one structural position is exchanged in the mixing process and (ii) the number of anions (i.e. O^{2-}) is the same in the stoichiometric formula of both end-members. As this is not the case in equation 2, the magnetite oxidation reaction was reformulated as:

$$[Fe^{2+}_3\ Fe^{3+}_3]_{Oh}\ Fe^{3+}_{3\ Td}O^{2-}_{12} + 2\ H^+ \rightleftharpoons [Fe^{3+}_5\ \square]_{Oh}Fe^{3+}_{3\ Td}O^{2-}_{12} + Fe^{2+} + H_2 \quad (6)$$

It appears that equation 6 does not only assume a H^+-promoted dissolution process, but it combines it with a redox reaction, as an oxidative dissolution process.[22] Note that this reaction could also be formulated differently, e.g. by adding 0.5 O_2 to the left side, to form 1 H_2O on the right-hand side.

Tabulated Gibbs free energies of the bulk iron oxides ($\Delta G_{mm,bulk}$ and $\Delta G_{mt,bulk}$, Table S1) were used.[42] Additionally, surface free energies (referring to hydrated surfaces, γ_{mm} and γ_{mt} in J m^{-2}) of the end-member phases were adjusted to determine the ΔG of the maghemite and magnetite nanoparticles ($\Delta G_{mm,nano}$ and $\Delta G_{mt,nano}$), in order to precisely match the experimental solubility data.[43] Because particle size determined by TEM (Fig. 2a-d) and crystallite size previously determined by XRD[27] did not significantly vary in all our experiments, the surface area was assumed to remain constant in the calculations. Previous attempts to measure the surface area of 10 nm-size nanomagnetites were in excellent agreement with surface areas calculated from TEM average size.[15,28,29] Such observation was also made for other minerals such as calcite.[44] Presently, the surface area was calculated equal to 101 $m^2\ g^{-1}$, using the average particle size determined by TEM (10.3 nm) and the assumption that all magnetite particles are spherical in shape. The large Fe^{2+} solubility dataset produced in our study at various pH and R_{ini} was used to calibrate this model, discarding the results obtained at pH < 5 that are supposed to not reflect chemical equilibrium. The fitting exercise using the aqueous chemical speciation code Phreeplot (PHREEQC-Phreeplot coupling)[35,36] gave γ_{mt} = 0.52 ± 0.10 J m^{-2} and γ_{mm} = 0.57 ± 0.29 J m^{-2} consistent with literature data (0.79 ± 0.28 and 0.57 ± 0.10 J m^{-2}, respectively),[45] and we found that a single

View Article Online
DOI: 10.1039/D2EN00112H

Guggenheim parameter was sufficient to obtain a satisfactory match between model and data (Fig. 4). A negative value of a_0 = -5.49 ± 0.50 confirms the negative ΔG_{mix} previously reported from oxide melt solution calorimetry for 100-300 nm sized magnetites.[3] It demonstrates that non-stoichiometric magnetites are a very special type of solid-solution, in comparison to many other solid-solutions exhibiting positive ΔG_{mix}.[40,46] This may be explained by the fact that mixing of magnetite and maghemite involves generation of vacancies and electron transfer processes, rather than mixing of ionic species on a given crystallographic position.

3.5 Prediction of redox potential in magnetite suspensions.

In environmental systems, magnetite plays an important role on biogeochemical cycling of redox sensitive contaminants and, hence, their fate, bioavailability and toxicity. For instance, magnetite can (i) immobilize uranium by reducing the rather mobile U(VI) to less mobile U(IV)[8], (ii) reduce Cr(VI) or nitrobenzene to less toxic Cr(III) or aniline[7,10] or, conversely, (iii) reduce As(V) to a more toxic As(III)[9]. Therefore, the redox potential (E_H, reported versus the standard hydrogen electrode) in magnetite containing environmental systems is essential to predict the behavior and fate of contaminants. For this reason, E_H values were experimentally recorded in all experiments using a Pt electrode and our model was used to predict the corresponding E_H values. At pH < 7, when pH decreases, all nanomagnetites tend to exhibit the same stoichiometry (Fig. 4b), which leads to similar calculated E_H values (Fig. 5a), in agreement with experimental results. At these conditions, accurate E_H might be achieved thanks to the large amount of dissolved Fe^{2+} and the small size of the nanoparticles that could react with the electrode.[47] At pH > 7, the model generally predicts lower E_H values than measured (open symbols in Fig. 5a). At these conditions Fe^{2+} is retained in the solid phase and experimental E_H determination is less reliable.[48] Nevertheless, calculated E_H, from +30 mV (R_{ini} = 0.10) to -154 mV (R_{ini} = 0.50) at pH = 7.2, compared rather well with expected E_H values according to the U(VI)/U(IV) redox chemistry.[8] This further supports the reliability of the present model. Therefore, our results allow proposing a new pH-E_H predominance diagram of Fe in the magnetite-maghemite-H_2O system ([Fe_3O_4] = 0.5 g L^{-1}, 10 nm particles, in 10 mM NaCl) accounting for the formation of the solid-solution (Fig. 5b). The predominance field of quasi-stoichiometric magnetite (R_{eff} > 0.495) is rather narrow in the simulated conditions, restricted to circumneutral to alkaline pH (> 6-7 depending on the E_H).

View Article Online
DOI: 10.1039/D2EN00112H

4 Conclusion

This study investigates the solubility and the stoichiometry of 10 nm-sized magnetite under a wide range of environmentally relevant pH (4-9) and redox conditions. It demonstrates that nanosized magnetite particles are in fact not stable at pH < 7, even in the absence of O_2. Magnetite-maghemite solid solutions form due to the H^+-promoted dissolution of Fe(II) from magnetite. Our long-term kinetic investigations and XMCD measurements of the magnetite stoichiometry reveal two stages concerning Fe(II) release from magnetite. The first one is rather fast for 10 nm-sized particles and proceeds within less than 24h, if the pH is moderately acidic (pH ≥ 5) and the stoichiometry of the final magnetite-maghemite solid solution exceeds 0.1. The Fe(II) release process becomes much slower for $R_{eff} < 0.1$, and even slows down further as the Fe(II)-depleted outer rim grows thicker while the core shrinks.[21,39] Accordingly, we developed the first equilibrium model that could predict the stoichiometry of nanomagnetites exposed to various pH conditions, partially oxidized by H_2O_2 and subsequently recharged by dissolved Fe(II). The model was also shown to provide estimations of the E_H consistent with experimental results.

Because magnetite nanoparticles play a key role in the biogeochemical cycling of various organic and inorganic pollutants, affecting the mobility, redox transformation, and toxicity of various organic and inorganic pollutants, this model could be a powerful decision support tool for environmental remediation using magnetite nanoparticles, or to unravel their complex behavior in natural systems. This model could also be used for tuning the key properties of magnetite nanoparticles, and thus provide theoretical guidance for analyses and design of environmental, catalytic and biomedical reactions.

View Article Online
DOI: 10.1039/D2EN00112H

Acknowledgments

Funding: This work was supported by Campus France, Khon Kaen University (Thailand), the C-FACTOR project funded by ANR (project number ANR-18-CE01-0008), the SURFNANO project funded by the CNRS-INSU EC2CO program, the SynFeSol project funded by the Brittany Region (AAP TRANSFERT 2019) and the Institut Universitaire de France (IUF). Through the support of the GeOHeLiS analytical platform of Rennes University, this publication is also supported by the European Union through the European Regional Development Fund (FEDER), the French Ministry of Higher Education and Research, the French Region of Brittany and Rennes Metropole. The authors acknowledge the SOLEIL synchrotron for beamtime allocation at the DEIMOS beamline (proposal 20200250). The authors are grateful to V. Dorcet and L. Rault for the assistance in TEM experiments performed on the THEMIS platform (ScanMAT, UMS 2011 University of Rennes 1-CNRS; CPER-FEDER 2007–2014).

Authorship contribution: Phoomipat Jungcharoen: Writing - original draft, Data curation, Investigation, Visualization. Mathieu Pédrot: Data curation, Investigation, Writing - review & editing, Resources, Supervision, Project administration, Funding acquisition. Frank Heberling: Data curation, Writing - review & editing. Khalil Hanna: Writing - review & editing. Fadi Choueikani: Investigation, Data curation, Writing - review & editing. Charlotte Catrouillet: Investigation, Data curation, Writing - review & editing. Aline Dia: Writing - review & editing. Rémi Marsac: Data curation, Investigation, Writing - review & editing, Resources, Supervision, Project administration, Funding acquisition.

Competing interests: The authors declare that they have no competing interests.

View Article Online
DOI: 10.1039/D2EN00112H

References

1 R. M. Cornell and U. Schwertmann, *The Iron Oxides: Structure, Properties, Reactions, Occurences and Uses, Second Edition*, Wiley-VCH: Weinheim, 2003.

2 M. Usman, J. M. Byrne, A. Chaudhary, S. Orsetti, K. Hanna, C. Ruby, A. Kappler and S. B. Haderlein, Magnetite and Green Rust: Synthesis, Properties, and Environmental Applications of Mixed-Valent Iron Minerals, *Chem. Rev.*, 2018, **118**, 3251–3304.

3 K. I. Lilova, F. Xu, K. M. Rosso, C. I. Pearce, S. Kamali and A. Navrotsky, Oxide melt solution calorimetry of Fe2+-bearing oxides and application to the magnetite–maghemite (Fe3O4–Fe8/3O4) system, *American Mineralogist*, 2012, **97**, 164–175.

4 W. Kündig and R. Steven Hargrove, Electron hopping in magnetite, *Solid State Communications*, 1969, **7**, 223–227.

5 C. N. Lininger, N. W. Brady and A. C. West, Equilibria and Rate Phenomena from Atomistic to Mesoscale: Simulation Studies of Magnetite, *Acc. Chem. Res.*, 2018, **51**, 583–590.

6 J. M. Byrne, N. Klueglein, C. Pearce, K. M. Rosso, E. Appel and A. Kappler, Redox cycling of Fe(II) and Fe(III) in magnetite by Fe-metabolizing bacteria, *Science*, 2015, **347**, 1473–1476.

7 C. A. Gorski, J. T. Nurmi, P. G. Tratnyek, T. B. Hofstetter and M. M. Scherer, Redox Behavior of Magnetite: Implications for Contaminant Reduction, *Environ. Sci. Technol.*, 2010, **44**, 55–60.

8 D. E. Latta, C. A. Gorski, M. I. Boyanov, E. J. O'Loughlin, K. M. Kemner and M. M. Scherer, Influence of Magnetite Stoichiometry on UVI Reduction, *Environ. Sci. Technol.*, 2012, **46**, 778–786.

9 C.-H. Liu, Y.-H. Chuang, T.-Y. Chen, Y. Tian, H. Li, M.-K. Wang and W. Zhang, Mechanism of Arsenic Adsorption on Magnetite Nanoparticles from Water: Thermodynamic and Spectroscopic Studies, *Environ. Sci. Technol.*, 2015, **49**, 7726–7734.

10 M. L. Peterson, A. F. White, Brown Gordon E. and G. A. Parks, Surface Passivation of Magnetite by Reaction with Aqueous Cr(VI): XAFS and TEM Results, *Environ. Sci. Technol.*, 1997, **31**, 1573–1576.

11 Z. Pan, B. Bártová, T. LaGrange, S. M. Butorin, N. C. Hyatt, M. C. Stennett, K. O. Kvashnina and R. Bernier-Latmani, Nanoscale mechanism of UO 2 formation through uranium reduction by magnetite, *Nature Communications*, 2020, **11**, 4001.

12 L. Gao, J. Zhuang, L. Nie, J. Zhang, Y. Zhang, N. Gu, T. Wang, J. Feng, D. Yang, S. Perrett and X. Yan, Intrinsic peroxidase-like activity of ferromagnetic nanoparticles, *Nature Nanotech*, 2007, **2**, 577–583.

13 R. A. Revia and M. Zhang, Magnetite nanoparticles for cancer diagnosis, treatment, and treatment monitoring: recent advances, *Materials Today*, 2016, **19**, 157–168.

14 Z. R. Stephen, F. M. Kievit and M. Zhang, Magnetite nanoparticles for medical MR imaging, *Materials Today*, 2011, **14**, 330–338.

15 W. Cheng, R. Marsac and K. Hanna, Influence of Magnetite Stoichiometry on the Binding of Emerging Organic Contaminants, *Environ. Sci. Technol.*, 2018, **52**, 467–473.

16 D. Faivre and T. U. Godec, From Bacteria to Mollusks: The Principles Underlying the Biomineralization of Iron Oxide Materials, *Angewandte Chemie International Edition*, 2015, **54**, 4728–4747.

17 V. Polshettiwar, R. Luque, A. Fihri, H. Zhu, M. Bouhrara and J.-M. Basset, Magnetically Recoverable Nanocatalysts, *Chem. Rev.*, 2011, **111**, 3036–3075.

18 S. Laurent, D. Forge, M. Port, A. Roch, C. Robic, L. Vander Elst and R. N. Muller, Magnetic Iron Oxide Nanoparticles: Synthesis, Stabilization, Vectorization, Physicochemical Characterizations, and Biological Applications, *Chem. Rev.*, 2008, **108**, 2064–2110.

19 I. A. M. Ahmed and B. A. Maher, Identification and paleoclimatic significance of magnetite nanoparticles in soils, *PNAS*, 2018, **115**, 1736–1741.

20 A. Kobayashi, M. Horikawa, J. L. Kirschvink and H. N. Golash, Magnetic control of heterogeneous ice nucleation with nanophase magnetite: Biophysical and agricultural implications, *PNAS*, 2018, **115**, 5383–5388.

View Article Online
DOI: 10.1039/D2EN00112H

21 J.-P. Jolivet and E. Tronc, Interfacial electron transfer in colloidal spinel iron oxide. Conversion of Fe3O4-γFe2O3 in aqueous medium, *Journal of Colloid and Interface Science*, 1988, **125**, 688–701.
22 K. Yuan, S. S. Lee, W. Cha, A. Ulvestad, H. Kim, B. Abdilla, N. C. Sturchio and P. Fenter, Oxidation induced strain and defects in magnetite crystals, *Nat Commun*, 2019, **10**, 1–10.
23 A. F. White, M. L. Peterson and M. F. Hochella, Electrochemistry and dissolution kinetics of magnetite and ilmenite, *Geochimica et Cosmochimica Acta*, 1994, **58**, 1859–1875.
24 F. H. Sweeton and C. F. Baes, The solubility of magnetite and hydrolysis of ferrous ion in aqueous solutions at elevated temperatures, *The Journal of Chemical Thermodynamics*, 1970, **2**, 479–500.
25 N. Morelová, N. Finck, J. Lützenkirchen, D. Schild, K. Dardenne and H. Geckeis, Sorption of americium / europium onto magnetite under saline conditions: Batch experiments, surface complexation modelling and X-ray absorption spectroscopy study, *Journal of Colloid and Interface Science*, 2020, **561**, 708–718.
26 S. P. Schwaminger, P. F. García, G. K. Merck, F. A. Bodensteiner, S. Heissler, S. Günther and S. Berensmeier, Nature of Interactions of Amino Acids with Bare Magnetite Nanoparticles, *J. Phys. Chem. C*, 2015, **119**, 23032–23041.
27 P. Jungcharoen, M. Pédrot, F. Choueikani, M. Pasturel, K. Hanna, F. Heberling, M. Tesfa and R. Marsac, Probing the effects of redox conditions and dissolved Fe2+ on nanomagnetite stoichiometry by wet chemistry, XRD, XAS and XMCD, *Environ. Sci.: Nano*, 2021, **8**, 2098–2107.
28 E. Demangeat, M. Pédrot, A. Dia, M. Bouhnik-le-Coz, F. Grasset, K. Hanna, M. Kamagate and F. Cabello-Hurtado, Colloidal and chemical stabilities of iron oxide nanoparticles in aqueous solutions: the interplay of structural, chemical and environmental drivers, *Environ. Sci.: Nano*, 2018, **5**, 992–1001.
29 R. Marsac, M. Pasturel and K. Hanna, Reduction Kinetics of Nitroaromatic Compounds by Titanium-Substituted Magnetite, *J. Phys. Chem. C*, 2017, **121**, 11399–11406.
30 W. B. Fortune and M. G. Mellon, Determination of Iron with o-Phenanthroline: A Spectrophotometric Study, *Ind. Eng. Chem. Anal. Ed.*, 1938, **10**, 60–64.
31 C. A. Gorski and M. M. Scherer, Influence of Magnetite Stoichiometry on Fe ^{II} Uptake and Nitrobenzene Reduction, *Environ. Sci. Technol.*, 2009, **43**, 3675–3680.
32 C. A. Gorski and M. M. Scherer, Determination of nanoparticulate magnetite stoichiometry by Mössbauer spectroscopy, acidic dissolution, and powder X-ray diffraction: A critical review, *American Mineralogist*, 2010, **95**, 1017–1026.
33 P. Ohresser, E. Otero, F. Choueikani, K. Chen, S. Stanescu, F. Deschamps, T. Moreno, F. Polack, B. Lagarde, J.-P. Daguerre, F. Marteau, F. Scheurer, L. Joly, J.-P. Kappler, B. Muller, O. Bunau and Ph. Sainctavit, DEIMOS: A beamline dedicated to dichroism measurements in the 350–2500 eV energy range, *Review of Scientific Instruments*, 2014, **85**, 013106.
34 K. Sartori, G. Cotin, C. Bouillet, V. Halté, S. Bégin-Colin, F. Choueikani and B. P. Pichon, Strong interfacial coupling through exchange interactions in soft/hard core–shell nanoparticles as a function of cationic distribution, *Nanoscale*, 2019, **11**, 12946–12958.
35 D. L. Parkhurst and C. A. J. Appelo, *User's guide to PHREEQC (Version 2): a computer program for speciation, batch-reaction, one-dimensional transport, and inverse geochemical calculations*, Water-resources Investigation Report 99–4259. USGS, Denver, Colorado., 1999.
36 D. G. Kinniburgh and D. M. Cooper, PhreePlot: Creating graphical output with PHREEQC, http://www.phreeplot.org/, (accessed 25 April 2020).
37 J.-P. Jolivet, C. Chanéac and E. Tronc, Iron oxide chemistry. From molecular clusters to extended solid networks, *Chem. Commun.*, 2004, 481–483.
38 E. Pellegrin, M. Hagelstein, S. Doyle, H. O. Moser, J. Fuchs, D. Vollath, S. Schuppler, M. A. James, S. S. Saxena, L. Niesen, O. Rogojanu, G. A. Sawatzky, C. Ferrero, M. Borowski, O. Tjernberg and N. B. Brookes, Characterization of Nanocrystalline γ-Fe2O3 with Synchrotron Radiation Techniques, *physica status solidi (b)*, 1999, **215**, 797–801.

View Article Online
DOI: 10.1039/D2EN00112H

39 Z.-X. Sun, F.-W. Su, W. Forsling and P.-O. Samskog, Surface Characteristics of Magnetite in Aqueous Suspension, *Journal of Colloid and Interface Science*, 1998, **197**, 151–159.
40 P. D. Glynn and E. J. Reardon, Solid-solution aqueous-solution equilibria; thermodynamic theory and representation, *American Journal of Science*, 1990, **290**, 164–201.
41 J. Liu, Z. Sun, Y. Deng, Y. Zou, C. Li, X. Guo, L. Xiong, Y. Gao, F. Li and D. Zhao, Highly Water-Dispersible Biocompatible Magnetite Particles with Low Cytotoxicity Stabilized by Citrate Groups, *Angewandte Chemie International Edition*, 2009, **48**, 5875–5879.
42 R. J. Lemir, D. A. Palmer, P. Taylor and H. Schlenz, *Chemical Thermodynamics of Iron, Part 2*, OECD Publications, 2020.
43 T. Hiemstra, Formation, stability, and solubility of metal oxide nanoparticles: Surface entropy, enthalpy, and free energy of ferrihydrite, *Geochimica et Cosmochimica Acta*, 2015, **158**, 179–198.
44 F. Heberling, L. Paulig, Z. Nie, D. Schild and N. Finck, Morphology Controls on Calcite Recrystallization, *Environ. Sci. Technol.*, 2016, **50**, 11735–11741.
45 A. Navrotsky, C. Ma, K. Lilova and N. Birkner, Nanophase Transition Metal Oxides Show Large Thermodynamically Driven Shifts in Oxidation-Reduction Equilibria, *Science*, 2010, **330**, 199–201.
46 P. Glynn, Solid-Solution Solubilities and Thermodynamics: Sulfates, Carbonates and Halides, *Reviews in Mineralogy and Geochemistry*, 2000, **40**, 481–511.
47 E. Silvester, L. Charlet, C. Tournassat, A. Géhin, J.-M. Grenèche and E. Liger, Redox potential measurements and Mössbauer spectrometry of FeII adsorbed onto FeIII (oxyhydr)oxides, *Geochimica et Cosmochimica Acta*, 2005, **69**, 4801–4815.
48 D. K. Nordstrom and K. M. Campbell, in *Treatise on Geochemistry (Second Edition)*, eds. H. D. Holland and K. K. Turekian, Elsevier, Oxford, 2014, pp. 27–68.

View Article Online
DOI: 10.1039/D2EN00112H

Figures and Tables

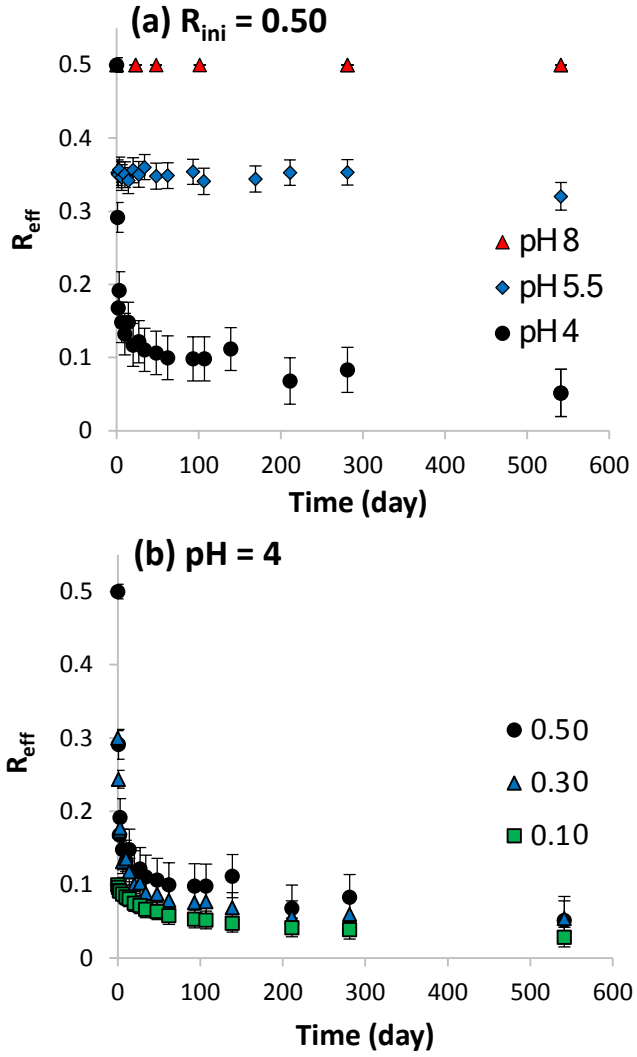

Figure 1. Long term kinetic experiments. (a) Transformation kinetics of stoichiometric magnetite (R_{ini} = 0.50) to magnetite-maghemite solid-solution at different pH values (4, 5.5 and 8). (b) Impact of magnetite initial stoichiometry (R_{ini} = 0.10, 0.30 and 0.50) on its transformation kinetics at pH 4.

View Article Online
DOI: 10.1039/D2EN00112H

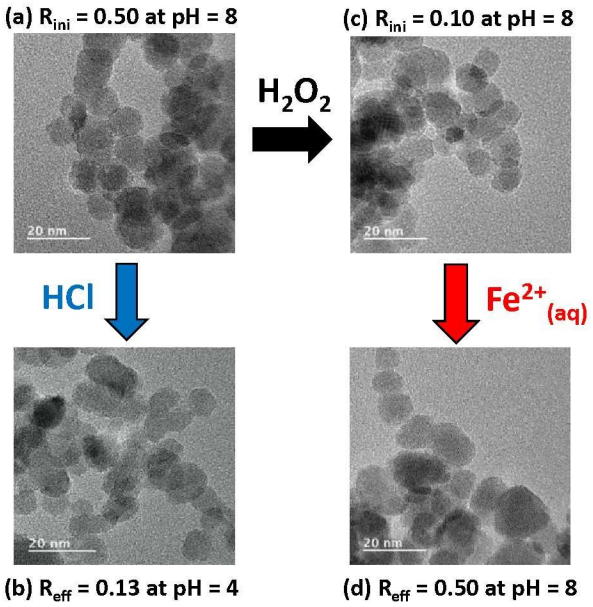

Figure 2. TEM characterization of magnetite reaction products with H^+, H_2O_2 or Fe^{2+}. (a-d) TEM images of the pristine magnetite (R_{ini} = 0.50) equilibrated at pH = 8 (a) or pH = 4 (R_{eff} = 0.13; b) during 20 days, or oxidized with H_2O_2 (R_{ini} = 0.10; c) followed by the addition of $Fe^{2+}_{(aq)}$ (R_{eff} = 0.50; d).

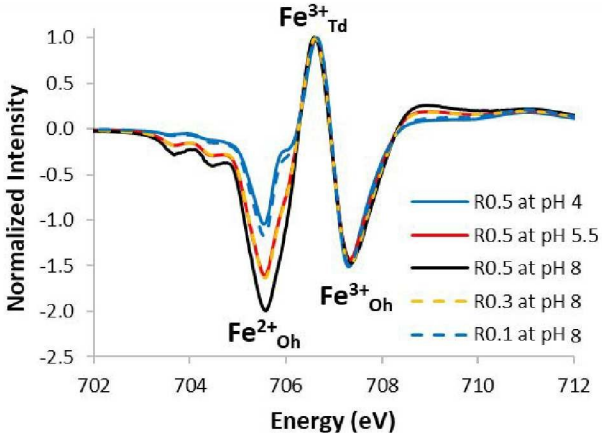

Figure 3. Normalized XMCD spectra of stoichiometric magnetite (R0.5) equilibrated at different pH values (4, 5.5 and 8) during 20 days as compared with stoichiometric maghemite oxidized by H_2O_2 (R0.1 and R0.3) at pH 8.

View Article Online
DOI: 10.1039/D2EN00112H

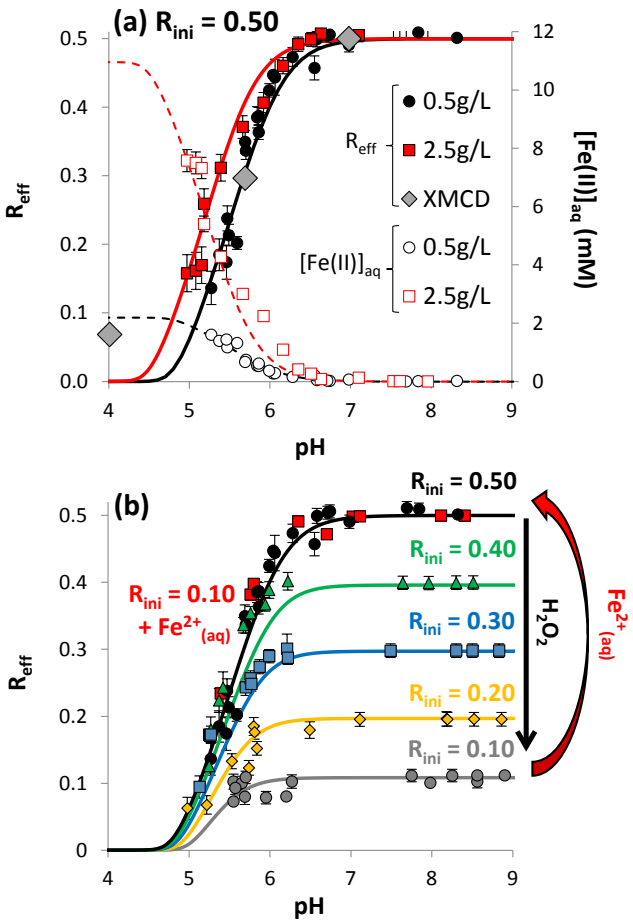

Figure 4. Magnetite stoichiometry under the influence of pH and redox conditions. (a) Effect of pH (4-9) and magnetite concentration (0.5 and 2.5 g L^{-1}) on Fe(II) solubility (open symbols) and corresponding magnetite effective stoichiometry (for R_{ini} = 0.50; full symbols). Large diamonds correspond to R_{eff} determined by X-ray magnetism circular dichroism (XMCD). (b) Effect of pH on R_{eff} for magnetites exhibiting different initial stoichiometries ($0.10 \leq R_{ini} \leq 0.50$), and of a non-stoichiometric magnetite (R_{ini} = 0.10) to which dissolved Fe(II) was added in order to reach an overall (solid+solution) Fe(II)/Fe(III) ratio of 0.50. Lines are modeling results, with the same color as the corresponding experimental data.

View Article Online
DOI: 10.1039/D2EN00112H

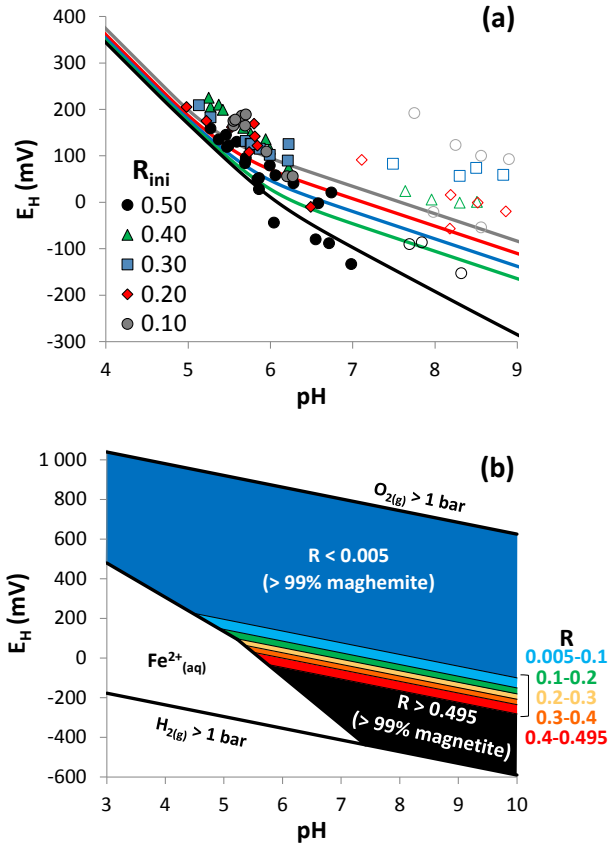

Figure 5. Relationships between pH, E_H and magnetite stoichiometry. (a) Effect of pH on measured and calculated redox potential in nanomagnetite suspensions ($0.10 \leq R_{ini} \leq 0.50$). (b) pH-$E_H$ predominance diagram of Fe in the magnetite-maghemite-H_2O system (10-nm-sized nanoparticles, $[Fe_3O_4] = 0.5$ g L^{-1} corresponding to 6.5 mM Fe, in 10 mM NaCl).